Original Article

Clinical Significance of Apurinic/Apyrimidinic Endodeoxyribonuclease 1 and MicroRNA Axis in Hepatocellular Carcinoma

Giovanna Mangiapane[1#] , Devis Pascut[2#] , Emiliano Dalla[1#] , Giulia Antoniali[1] , Monica Degrassi[1] , Lory Saveria Crocè[2,3,4] , Veronica De Sanctis[5] , Silvano Piazza[6] , Giulia Canarutto[6] , Claudio Tiribelli[2] and Gianluca Tell[1*]

[1]Laboratory of Molecular Biology and DNA Repair, Department of Medicine, University of Udine, Udine, Italy; [2]Fondazione Italiana Fegato - ONLUS, Liver Cancer Unit, Trieste, Italy; [3]Department of Medical Sciences, University of Trieste, Trieste, Italy; [4]Clinica Patologie Fegato, Azienda Sanitaria Universitaria Giuliano Isontina (ASUGI), Trieste, Italy; [5]NGS Core Facility, Department CIBIO, University of Trento, Trento, Italy; [6]Computational Biology, International Centre for Genetic Engineering and Biotechnology, ICGEB, Trieste, Italy

Abstract

Background and Aims: Identification of prognostic factors for hepatocellular carcinoma (HCC) opens new perspectives for therapy. Circulating and cellular onco-miRNAs are noncoding RNAs which can control the expression of genes involved in oncogenesis through post-transcriptional mechanisms. These microRNAs (miRNAs) are considered novel prognostic and predictive factors in HCC. The apurinic/apyrimidinic endodeoxyribonuclease 1 (APE1) contributes to the quality control and processing of specific onco-miRNAs and is a negative prognostic factor in several tumors. The present work aims to: a) define APE1 prognostic value in HCC; b) identify miRNAs regulated by APE1 and their relative target genes and c) study their prognostic value. ***Methods:*** We used The Cancer Genome Atlas (commonly known as TCGA) data analysis to evaluate the expression of APE1 in HCC. To identify differentially-expressed miRNAs (DEmiRNAs) upon APE1 depletion through specific small interfering RNA, we used NGS and nanostring approaches in the JHH-6 HCC tumor cell line. Bioinformatics analyses were performed to identify signaling pathways involving APE1-regulated miRNAs. Microarray analysis was performed to identify miRNAs correlating with serum APE1 expression. ***Results:*** APE1 is considerably overexpressed in HCC tissues compared to normal liver, according to the TCGA-liver HCC (known as LIHC) dataset. Enrichment analyses showed that APE1-regulated miRNAs are implicated in signaling and metabolic pathways linked to cell proliferation, transformation, and angiogenesis, identifying Cyclin Dependent Kinase 6 and Lysosomal Associated Membrane Protein 2 as targets. miR-33a-5p, miR-769, and miR-877 are related to lower overall survival in HCC patients. Through array profiling, we identified eight circulating DE-miRNAs associated with APE1 overexpression. A training phase identified positive association between sAPE1 and miR-3180-3p and miR-769. ***Conclusions:*** APE1 regulates specific miRNAs having prognostic value in HCC.

Introduction

Hepatocellular carcinoma (HCC) is the most common type of liver cancer. Over 90% of HCC cases are associated with chronic liver diseases.[1] Cirrhosis, along with hepatitis B virus or hepatitis C virus infections, is one of the major risk factors in HCC.[2,3] Other risk factors include alcohol consumption, obesity-related nonalcoholic steatohepatitis, or diabetes.[1] Different etiologies, along with genotoxic insults, contribute to the pathogenesis of HCC,[1] and, currently, the diagnosis with noninvasive methods is challenged by the lack of molecular information. Although driver mutations for HCC have been identified, involving for example *Tumor Protein P53 (TP53)*, *Telomerase Reverse Transcriptase (TERT)*, and *Catenin Beta 1 (CTNNB1)* genes,[4] these are still untreatable and combination therapies are under investigation to improve the efficacy of existing treatments.[1,5]

Genome instability resulting from dysfunctional DNA damage response is a common characteristic of HCC, leading to poor anticancer treatment efficacy and the development of chemotherapy resistance mechanisms.[6–8] Endogenous or

exogenous agents, including chemotherapeutic drugs, can determine alkylation or oxidative DNA damage, which is repaired by the base excision repair pathway.[9] The apurinic/apyrimidinic endodeoxyribonuclease 1 (APE1) is the main AP-endonuclease of base excision repair and it also plays non canonical functions such as regulation of transcription factors, monitoring redox homeostasis, and participating in the stability and metabolism of RNAs, including micro microRNAs (miR-NAs).[10,11] APE1 overexpression is a predictive factor in many tumor types including ovarian, lung, neurologic, and hepatic cancers and it is often present in both nuclear and cytosolic compartments. APE1 overexpression has been linked to chemoresistance in non-small cell lung cancer and HCC.[10,12]

Several APE1 interactors contribute to the regulation of its multifunctional activities, promoting chemoresistance, tumor progression, and miRNA processing.[13,14] Recently, we and others found that the down-regulation of APE1 alters the expression of certain miRNAs in osteosarcoma and lung cancer cells.[13,15,16] Moreover, our laboratory identified APE1 as a partner of Drosha during the processing of precursor forms of oncomiR-221 and 222 in response to oxidative stress in cervical cancer.[13] This unexpected function may have important implications due to the well-known role of miRNAs as biomarkers, especially as circulating biomarkers. The participation of miRNAs in a broad range of cellular processes under pathological conditions[17] such as cell proliferation, differentiation as well as tumorigenesis, metastasis, and chemoresistance, makes circulating miRNAs particularly attractive for studies aiming to identify disease-related molecules having a diagnostic or even a prognostic role.

In recent years, the extracellular release of APE1 has opened up a new field of study on the biological functions of this DNA repair enzyme in the extracellular compartment. Serum APE1 (sAPE1) has emerged as a biomarker for the detection and prognosis of different cancers,[18] as well as for predicting lymph node metastasis.[19] In the context of non-small cell lung cancer, sAPE1 is considered a prognostic factor, and its levels have been associated with worse progression-free survival.[20] Our recent study has confirmed that sAPE1 level is also a prognostic factor for HCC and can distinguish between cancer and cirrhotic patients.[21] Moreover, we have shown that APE1 is released through exosomes in mammalian cell lines and that genotoxic stress promotes its cellular secretion, providing new insights into its noncanonical functions and its contribution to tumor biology.[22] In this study, we identified novel miRNAs regulated by APE1 in HCC and we investigated their prognostic value in this disease.

Methods

Study design

To identify miRNAs regulated by APE1 in HCC, the study was organized as follows:

- *In vitro discovery phase*: The miRNome profiling was analyzed in JHH-6 cells following the transient APE1 silencing to identify DEmiRNAs candidates.
- *In vivo discovery phase*: The comparison between the serum miRNome profiling of patients with high sAPE1 vs. patients with low sAPE1, was used to identify serum miR-NAs associated with sAPE1 levels.

Cell lines used and transient transfections with small interfering RNA (siRNA) and RNA extraction

JHH-6 hepatocarcinoma cells[23] were grown in William's medium E (Sigma-Aldrich, St. Louis, MO, USA). Huh7 differentiated hepatocytes derived from cellular carcinoma,[24] HepG2 differentiated hepatocellular carcinoma cells,[25] and HCT-116 cells were grown in Dulbecco's modified Eagle's medium (EuroClone, Milan, Italy). A549 cells were grown in RPMI medium (Euroclone, Milan, Italy). All media were supplemented with 10% fetal bovine serum (Euroclone), 2 mM L-glutamine (Euroclone), 100 U/mL penicillin, and 100 mg/mL streptomycin. Cells were negative for mycoplasma. The tests were performed with N-GARDE Mycoplasma PCR Reagent (Euroclone).

Cells were seeded in the number of 1.0×10^6 in a 10 cm dish. The following day, transfection was performed using 100 pmol of custom hAPE1 siRNA or with nontargeting siRNA pool (siSCR) as a control (GE Healthcare Dharmacon, Lafayette, CO, USA). The DharmaFECT transfection reagent (GE Healthcare Dharmacon) was employed for transfection following the manufacturer's protocols. Two days after transfection, cells were collected, and whole cell extracts and RNA were prepared. RNA extraction was carried out using miRNeasy kit (Qiagen, Germantown, MD, USA) following the manufacturer's protocols.

RNAseq and nanostring nCounter miRNA expression profiling

miRNA expression profiling through RNAseq and the nanostring nCounter system were performed in total RNA samples collected from JHH-6 silenced for APE1 and their respective siSCR controls, as previously reported.[16]

Pathway enrichment analysis of validated miRNA targets

The validated targets of the identified DEmiRNAs were defined using the DIANA-MirPath v.3 web-server.[26] Enriched pathways analysis was performed querying the Gene Ontology – Biological Process databases ($p \leq 0.05$), employing the gene union and pathway union methods. To improve the biological relevance of the results, a network representation was generated by using the Kyoto Encyclopedia of Genes and Genomes (KEGG)-PathwayConnector,[27] sorted by adjusted p-value in ascending order. Ten EnrichR pathways were analyzed.

ClueGO data analysis

Enriched pathways associated with target genes expressed with inverse correlation to the identified miRNAs were identified using the Cytoscape app ClueGO. The queried datasets were CLINVAR_Human-diseases, CORUM_CORUM-3.0-FunCat-MIPS, Gene Ontology (GO)_BiologicalProcess (last accessed: May 8, 2020), GO_ImmuneSystemProcess, KEGG, Reactome (reactions and pathways) and WikiPathways. Applied statistics involved enrichment/depletion (two-sided hypergeometric test) and correction was performed by Benjamini-Hochberg with p-value cutoff of 0.05, min/max GO level of 4/8, and minimum number of genes of 3/1 (A549/JHH-6).

Survival analysis

To determine the prognostic value of APE1 for overall survival (OS), we analyzed The Cancer Genome Atlas (TCGA)-Liver Hepatocellular Carcinoma (LIHC) dataset using Gene Expression Profiling Interactive Analysis 2 (GEPIA2) (http://http://gepia2.cancer-pku.cn/, accessed 21 January 2022), stratifying patients using the median cutpoint. For nanostring and RNAseq DEmiRNAs, as well as for the derived miRNA signatures, we downloaded transcriptomics (HiSeq, miRgene level; reads per million (RPM), Log2(Val+1)) and clinical data from the LinkedOmics portal for the TCGA-LIHC cohort (n=372 and n=377, respectively; http://linkedomics.org/data_download/TCGA-LIHC/). We then selected a final cohort of patients associated with clinical data (n=344) that was used for downstream analyses. We used the clinical,

RTCGA, and survival R packages to divide patients into high expression and low expression groups using the surv_cut-point function (applied minprop=0.33). We verified differences in OS between subgroups by applying a log-rank test (*p*-value <0.05) and summarizing data with Kaplan–Meier plots.

Gene expression profiling of DEmiRNA targets in cancer and normal datasets

We obtained transcriptomics data of APE1 and of the eight DEmiRNAs validated targets (Cyclin Dependent Kinase 6 (*CDK6*), CAMP Responsive Element Binding Protein Like 2 (*CREBL2*), Muscleblind Like Splicing Regulator 1 (*MBNL1*), Scm Polycomb Group Protein Like 1 (*SCML1*), Ankyrin Repeat Domain 52 (*ANKRD52*), Lysosomal Associated Membrane Protein 2 (*LAMP2*), Pantothenate Kinase 3 (*PANK*3), and Zinc Finger Homeobox 3t (*ZFHX3*)) from the TCGA-LIHC cancer dataset (*n*=369) and from normal data (matched TCGA and GTEx, *n*=160), using GEPIA2,[28] selecting expression analysis, expression DIY, box plots, and using the derived gene symbols in the gene A box. Boxplots were used to represent data (red: tumor; black: normal).

Preparation of cell extracts and western blot analysis

Whole cell extracts were made and quantified as previously described.[22] Western blot assays were performed with the following primary antibodies: anti-APE1 (13B8E5C2; Novus, Littleton, CO, USA) and anti-β-Tubulin (T0198; Sigma-Aldrich) for normalization. The secondary antibodies used were IRDye800 or IRDye600 labeled. Image acquisition and densitometry analysis were obtained with Odyssey CLx Infrared Imaging system (LI-COR, Lincoln, NE, USA).

Quantitative real-time PCR (qRT-PCR)

miRNA expression analysis was carried out by qRT-PCR using the *Taq*Man advanced miRNA assay (Life Technologies, Carlsbad, CA, USA). Briefly, 10 ng of total RNA were reverse transcribed with *Taq*Man advanced miRNA cDNA synthesis kits (Life Technologies, Carlsbad, CA, USA) or qScript microRNA cDNA synthesis kits (Quantabio, Beverly, MA, USA), following the manufacturer's protocols. qRT-PCR reactions were performed with *Taq*Man fast advanced master mix, or the PerfeCTa SYBR green supermix (Quantabio, Beverly, MA, USA) kits following the manufacturer's protocols and run with a CFX Touch real-time PCR System (Bio-Rad, Hercules, CA, USA). qRT-PCR analysis was performed with the ΔΔct method, using miR-16-5p as a reference. Cq values >45 were considered negative and melting point curves were used in all assays to check primer specificity.

DE-mRNA targets expression was analyzed with reverse transcription of 1 µg of total RNA with SensiFAST cDNA synthesis kits (Meridian Bioscience, Cincinnati, OH, USA) following the manufacturer's protocols and qRT-PCR reactions were performed using SYBR No-ROX kits following the manufacturer's protocols (Meridian Bioscience, Cincinnati, OH, USA). Primers were acquired from Sigma-Aldrich (Merck KGaA, Darmstadt, Germany). Assays were carried out as indicated above using Glyceraldehyde-3-Phosphate Dehydrogenase (GAPDH), Actin alpha, miR-1280, miR-1275, and 28S as reference genes. Expression levels were calculated using the 2-ΔΔCt formula.

In vivo training phase

miRNA candidates identified in the previous phases were assessed in the serum of 24 patients with HCC, 12 with high sAPE1 expression and 12 with low sAPE1 expression. The *in vivo* validation phase included miRNA candidates that were significantly correlated with sAPE1 expression in HCC patients and were assessed in the serum of 67 other HCC patients, 33 with high sAPE1 expression and 34 with low sAPE1 expression.

Patients

A total of 109 consecutive patients who were diagnosed with HCC according to the European Association for the Study of the Liver criteria,[29] were enrolled in the study and referred to the liver center between 2012 and 2018. Samples were collected at the time of HCC diagnosis. The clinical and demographic features of the groups are shown in Supplementary Table 1.

Ethical approval and consent to participate

Written informed consent was provided by all patients. The investigation was conducted following the principles in the Declaration of Helsinki. The study was approved by the regional ethical committee (Comitato Etico Regionale Unico FVG, No. 14/2012 ASUITS and Prot. No. 2018 Os-008-AS-UITS, CINECA No. 2225).

Serum collection, microarray profiling and data analysis

Serum collection and miRNA extraction were performed as previously described.[21,30] Small RNAs were extracted from the serum of HCC patients and independently profiled on an Affymetrix Genechip miRNA 3.0 (Thermo Fischer Scientific, Waltham, MA, USA) as previously described.[30] One-way analysis of variance was used to determine gene expression differences in the microarray results. The Benjamini-Hochberg method was used for multiple testing corrections, providing false discovery rate-corrected *p*-values.

HCC tissues collection and RNA extraction

We collected fresh hepatic tissues from untreated HCC patients undergoing liver resection. Specifically, samples included HCC nodule, peri-HCC, and surrounding liver cirrhosis. Tissues were snap-frozen and stored at −80°C. Total RNA was extracted using TriReagent (Merck KGaA, Darmstadt, Germany), according to manufacturer instructions.

sAPE1 quantification

sAPE1 levels were determined using Human APEX1 ELISA kit (Cusabio, Houston, TX, USA) as previously described.[21]

Data analysis and statistical methods

Mann-Whitney *U* tests were used to compare the differences between the two independent groups. The Kruskal–Wallis test, in a one-way analysis of variance procedure, was used for multiple comparisons. Differences in demographic characteristics were compared by applying the chi-square test. The relationship between sAPE and circulating miRNAs was analyzed by Pearson correlation analysis. The statistical analysis was performed with NCSS 11 software (2016, NCSS, LLC. Kaysville, UT, USA; ncss.com/software/ncss), Stata 16.0 (Stata Corporation, College Station, TX, USA), and Student's *t*-test using GraphPad Prism (https://www.graphpad.com/features). Differences were considered statistically significant when the *p*-value was <0.05.

Results

APE1 overexpression is associated with poor prognosis in HCC

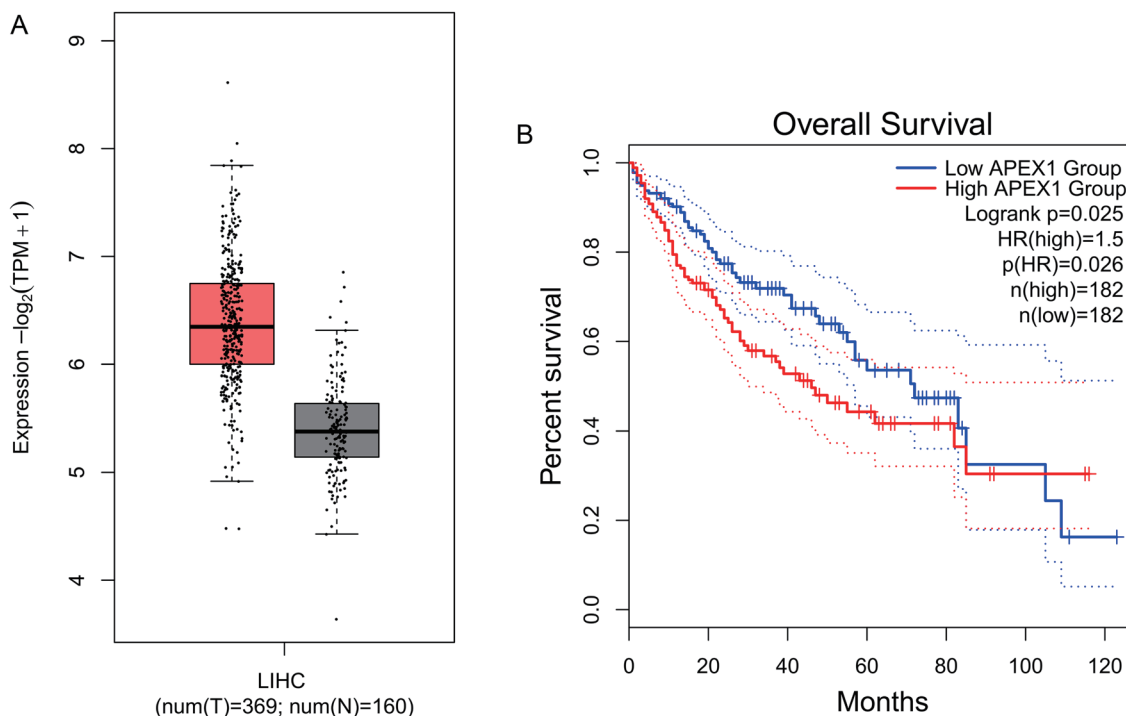Before investigating the potential role of APE1 in regulating

Fig. 1. Prognostic value of apurinic/apyrimidinic endodeoxyribonuclease 1 (APE1) in The Cancer Genome Atlas (TCGA) – Liver Hepatocellular Carcinoma (LIHC) patients. (A) Gene expression profiling of APE1 in the TCGA-LIHC dataset. Boxplot showing log2-transformed gene expression levels in the TCGA-LIHC (n=369) compared with matched TCGA normal and Genotype-Tissue Expression (GTEx) datasets (n=160). Red: tumor; black: normal. p<1e-05. (B) Prognostic value of APE1 in TCGA-LIHC patients. Kaplan–Meier plot of different overall survival (OS) rates of patients in high expression (red) and low expression (blue) groups, stratified by median APE1 expression (hazard ratio=1.5, p=0.026).

prognostic miRNAs in HCC, we evaluated the levels of APE1 expression in the TCGA-LIHC cohort[31] by comparing tumor (n=369) and matched normal tissues (n=50). To increase the statistical power, we also included the GTEx normal liver samples (n=110). We found that APE1 expression was significantly higher (p<1e-05) in tumors compared with normal tissues (Fig. 1A, red box plot). Subsequently, the TCGA-LIHC dataset was used to investigate the prognostic significance of APE1 for OS by categorizing patients into high- and low-expressing groups based on the median expression value of APE1. Results were presented through a Kaplan–Meier plot (Fig. 1B), which demonstrated a statistically significant difference in the OS rates between high-expressing (n=182) and low-expressing (n=182) patients, with the former having lower survival rates (hazard ratio=1.5, p=0.026).

miRNA expression analysis in HCC cancer cells upon APE1 depletion

After defining APE1 prognostic significance in HCC, we evaluated its role in regulating miRNA expression. Specifically, we transiently silenced JHH-6 hepatocellular carcinoma cells with a customized APE1 siRNA (siAPE1) and siRNA scramble control (siSCR) to identify DEmiRNAs (Fig. 2A). We performed both RNAseq [abs (log fold-change (FC)] ≥0.5, p≤0.05)] and nanostring [abs(logFC) ≥1.0, adjusted p≤0.1)] analyses. The RNAseq analysis revealed that only six miRNAs were differentially expressed upon APE1 depletion, with four miRNAs being significantly down-regulated in the APE1 knockdown cells (miR-let7c-5p, miR-877, miR-769, and miR-874) and two significantly up-regulated (miR-3609 and miR-6087, (Supplementary Table 2). From the nanostring analysis, we identified five up-regulated miRNAs (miR-2117, miR-1973, miR-1246,

miR-378e, and miR-575) and two down-regulated miRNAs (miR-99a-5p and miR-33a-5p; Supplementary Table 3). Unfortunately, no shared DEmiRNAs were identified when comparing the results of the two distinct analytical approaches used. The limited number of DEmiRNAs detected in both experiments, compared with our previous findings in HeLa and A549 cell lines,[13,16] may be attributed to the relatively weak silencing efficiency observed in the JHH-6 cell model (Fig. 2A).

Functional enrichment analysis of differently expressed miRNAs identifies gene targets associated with RNA metabolism and transport

We firstly performed a GO pathway enrichment analysis by considering the targets of DEmiRNAs identified through the nanostring analysis (validated subset), thus identifying terms associated with RNA biosynthesis/metabolism and regulation of gene expression (Fig. 2B). Similarly, we investigated the KEGG database and used the KEGG-PathwayConnector[27] web tool to generate a summarized network of the top 15 most enriched pathways, revealing 11 major nodes including the Hippo pathway, Wingless-related integration site (WNT) signaling, p53 pathway, and Forkhead Box O (FOXO) pathway (Fig. 2C). Interestingly, we observed the RNA transport pathway as one of the significantly enriched terms. We applied the same approach to the DEmiRNAs identified through RNAseq analysis, which yielded similar results from the GO database. Interestingly, miR-877-5p and miR-769-5p were found to be associated with innate immunity and blood coagulation (Fig. 3A). Additionally, the top 15 most enriched KEGG pathways (Fig. 3B) highlighted the role of APE1-regulated miRNAs in signaling and metabolic pathways associated with cell proliferation *(PhosphatidylInositol 3-Kinase (PI3K)/*
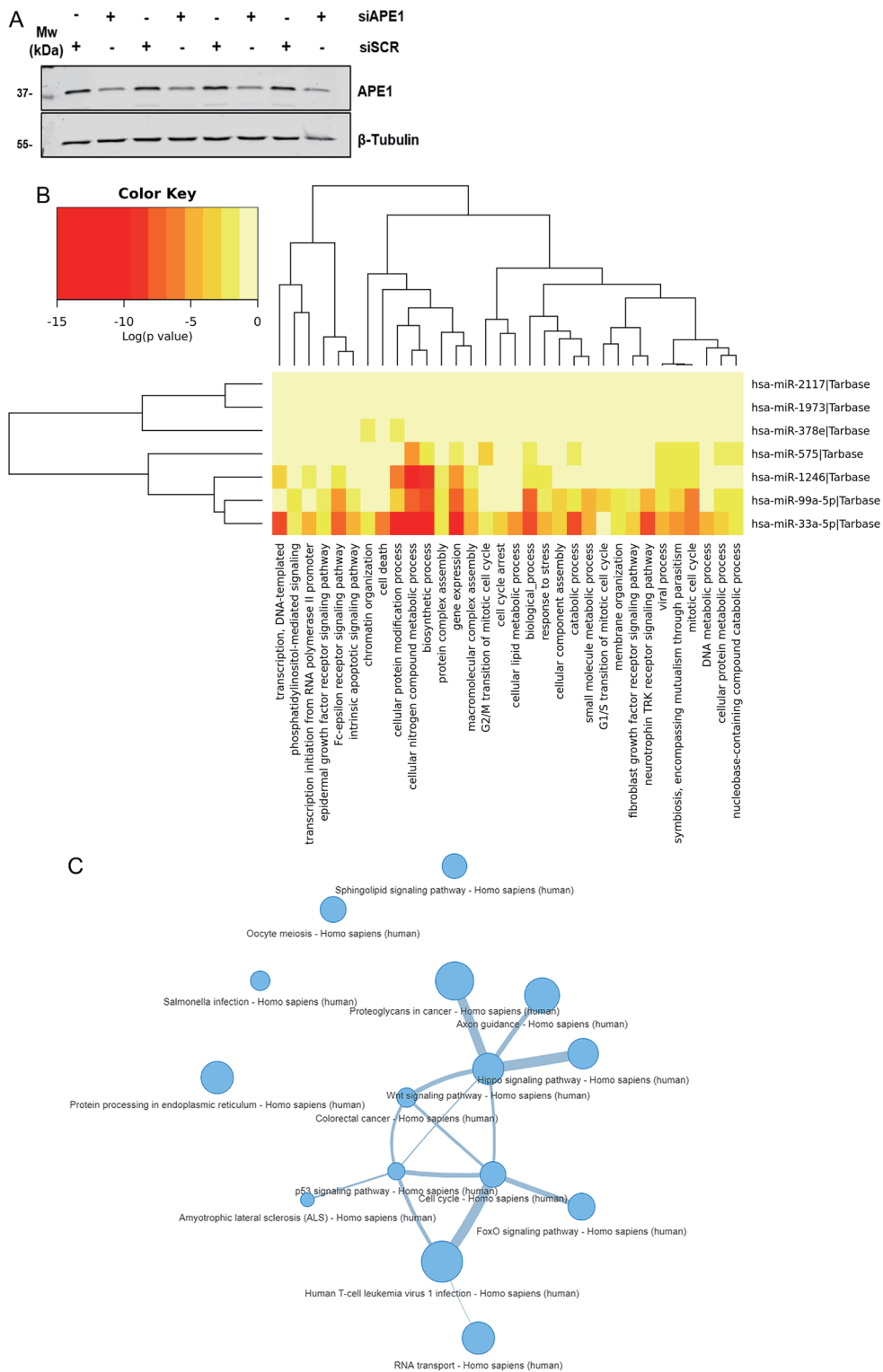
Fig. 2. Apurinic/apyrimidinic endodeoxyribonuclease 1 (APE1) regulates microRNAs (miRNAs) associated with RNA metabolism and transport. (A) Western blotting assays of JHH-6 cells silenced for APE1 (siAPE1) or silenced using a small interfering RNA (siRNA) scramble as control (siSCR). The upper panel shows the detection of APE1 (predicted molecular weight 37 kDa). β-Tubulin (predicted molecular weight 55 kDa) was used as the loading control (lower panel). The assays were performed in quadruplicate. (B) Functional enrichment analysis of differentially-expressed microRNA (DEmiRNA) validated targets. Heatmap of significantly enriched functional terms (adjusted $p \leq 0.05$) associated with DEmiRNAs validated targets, according to DIANA-MirPath (Gene Ontology biological process). Enriched terms and miRNAs are clustered, based on the log (adjusted *p*-value). (C) Functional enrichment analysis of DEmiRNAs validated targets. Network of the top 15 enriched Kyoto Encyclopedia of Genes and Genomes (KEGG) functional terms ($p \leq 0.05$) associated with DEmiRNAs validated targets using the KEGG-PathwayConnector web tool.
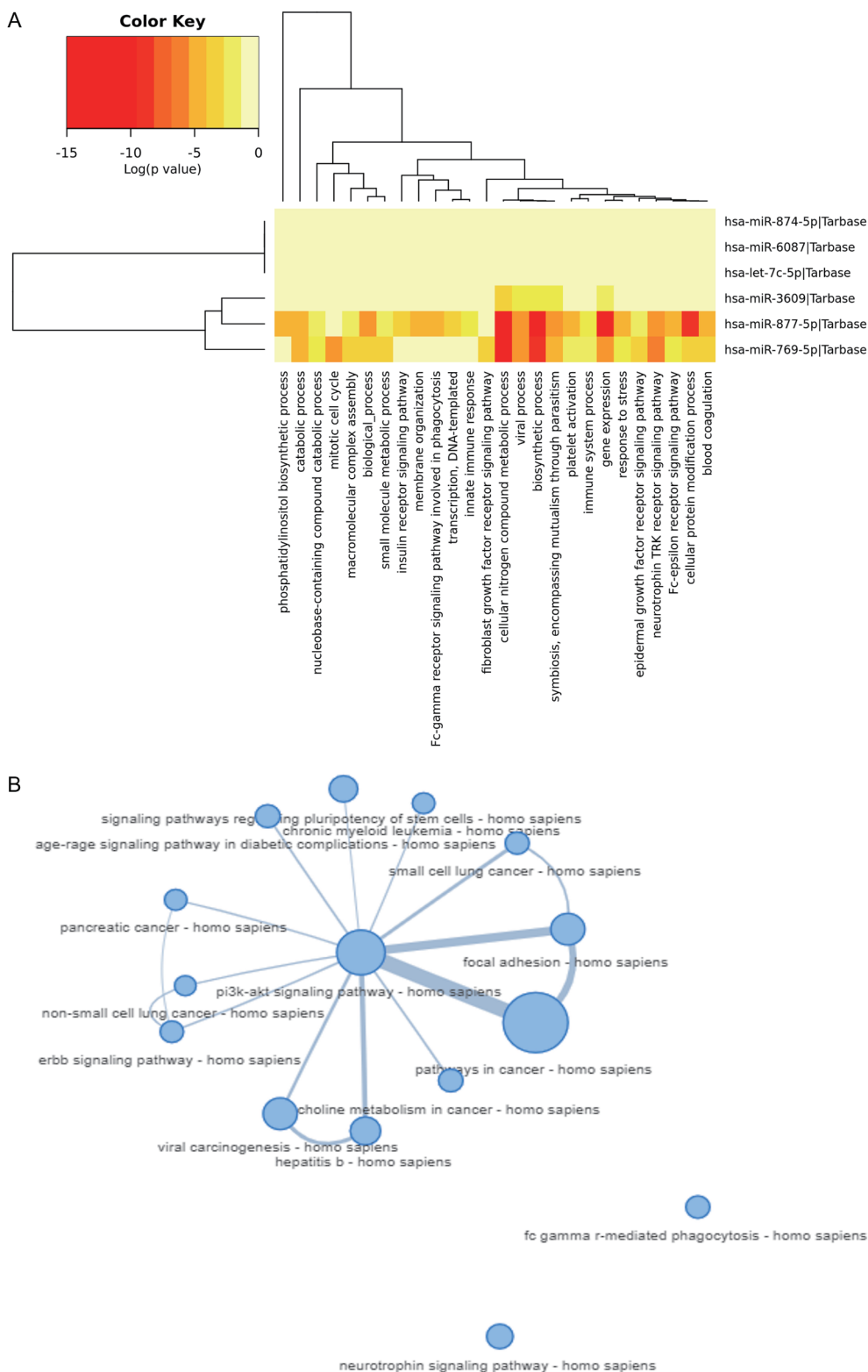
Fig. 3. Apurinic/apyrimidinic endodeoxyribonuclease 1 (APE1) regulates microRNA (miRNAs) related to cancer. (A) Functional enrichment analysis of RNAseq differentially-expressed microRNA (DEmiRNAs) validated targets. Heatmap showing the significantly enriched functional terms (adjusted $p \leq 0.05$) associated with DEmiRNAs validated targets according to DIANA-MirPath (GO biological process). Enriched terms and miRNAs are clustered, based on the log (adjusted p-value). (B) Functional enrichment analysis of RNAseq DEmiRNAs validated targets. Network of the top 15 enriched KEGG functional terms ($p \leq 0.05$) associated with DEmiRNAs validated targets according to the Kyoto Encyclopedia of Genes and Genomes (KEGG)-PathwayConnector web tool.
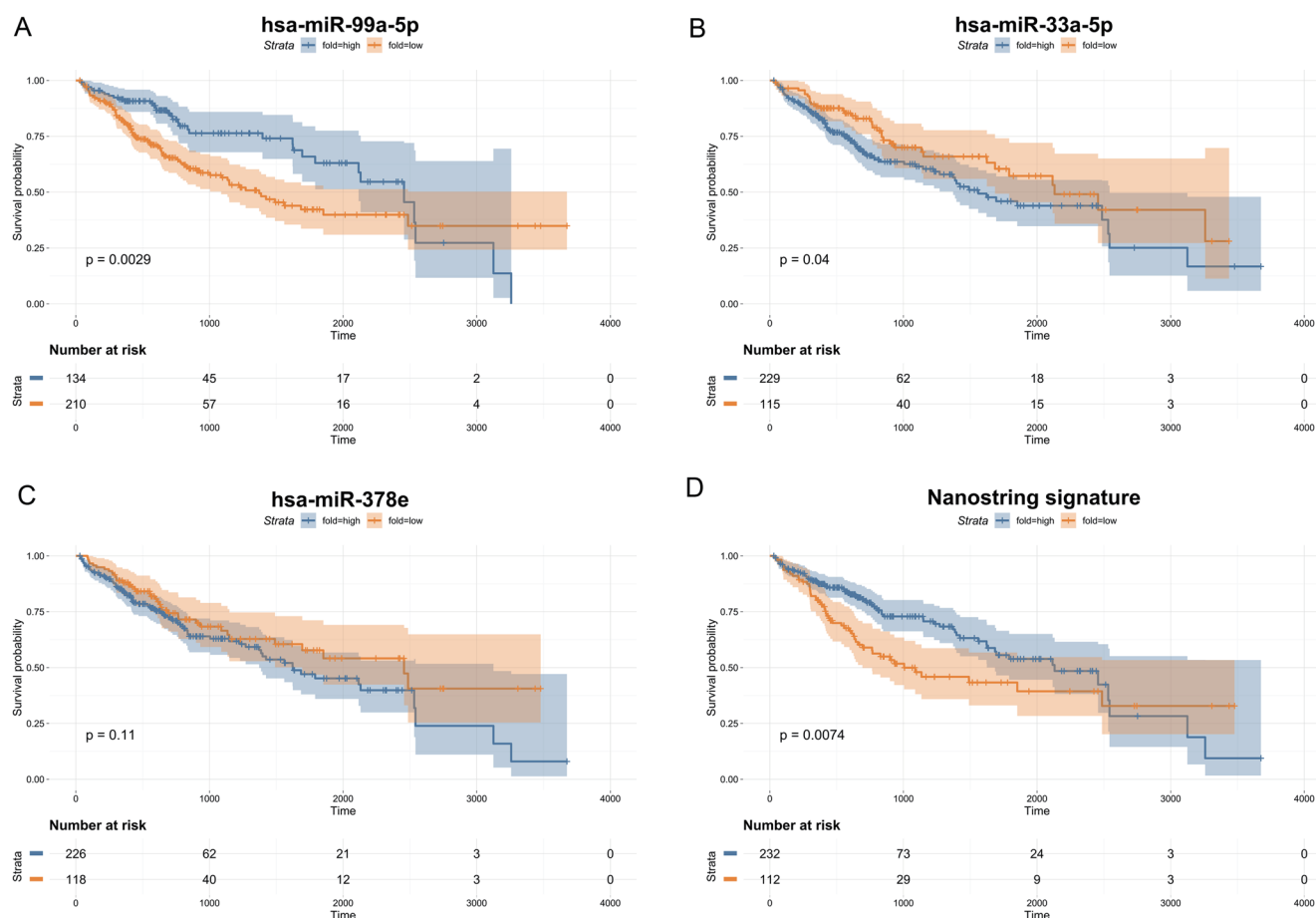
Fig. 4. Prognostic value of the nanostring microRNA signature in The Cancer Genome Atlas (TCGA) - Liver Hepatocellular Carcinoma (LIHC) patients. (A-D) Kaplan–Meier plots of miR-99a-5p (A), miR-33a-5p (B), miR-378e (C) and the whole-signature (D) overall survival (OS) rates of patients in high expression (blue) and low expression (orange) groups stratified by *p*-value optimization of the miRNA signature.

Ak strain transforming (AKT);[32] choline metabolism[33], transformation (*Epidermal growth factor* signaling *(ERBB)* signaling[34]) and angiogenesis (Advanced glycation endproducts *(AGEs)- Receptor for advanced glycation endproducts (RAGE)* signaling[35]). The results emphasize a role of APE1 in regulating oncogenic and proliferative processes, as well as its involvement in the negative regulation of the apoptotic process, DNA damage response signaling, cellular processes related to mRNA processing, regulation of RNA biosynthetic process, mRNA export from the nucleus and RNA transport and vesicle-mediated transport.

Prognostic significance of APE1-regulated miRNA signatures

After defining the predictive potential of APE1, we investigated whether differently expressed miRNA signatures regulated by APE1 could also serve as prognostic factors. We initially considered the nanostring-derived data, but its informative power was hindered owing to the limited availability of complete transcriptomics and survival information for only three out of the seven DEmiRNAs (miR-378e, miR-99a-5p, and miR-33a-5p). Nevertheless, we stratified patients by *p*-value optimization, finding that miR-99a-5p and miR-33a-5p were both able to significantly differentiate patients, with miR-99a-5p overexpression associated with a favorable prognosis (*p*=2.9e-03; Fig. 4A), while the opposite was observed for

miR-33a-5p (*p*=4e-02; Fig. 4B). For miR-378e, the trend was similar to that of miR-33a-5p, although the differences were not statistically significant (Fig. 4C). We finally considered the three miRNA signatures where higher values were associated with longer OS (*p*=7.4e-03; Fig. 4D). The same approach was used for the miRNAseq-derived data. The presence of a more complete dataset allowed us to obtain more consistent results between the single miRNAs and the complete signature, except for miR-6087 which was not associated to any clinical or expression data. Indeed, the low expression of four out of five miRNAs (Fig. 5A, B, D, E) was associated with a better outcome, although only miR-769 (*p*=1.2e-04) and miR-877 (*p*=2.8e-03) were statistically significant. Only miR-let-7c had the opposite trend (*p*=9.7e-03; Fig. 5C). Consistently, lower values of the DEmiRNA signature were associated with a favorable patient outcome (*p*=0.016; Fig. 5F). Results suggest the association of the down-regulated miRNAs upon APE1 silencing with a better prognosis, thus corroborating the hypothesis of the existence of an APE1-miRNAs axis that promotes and sustains oncogenesis in HCC, leading to a worse prognosis and reduced OS.

Validation of high-throughput analysis results in APE1-depleted RNA pools of JHH-6

After defining the prognostic value of APE1 and its DEmiRNAs in HCC, we validated the results by qRT-PCR in a JHH-6 APE1
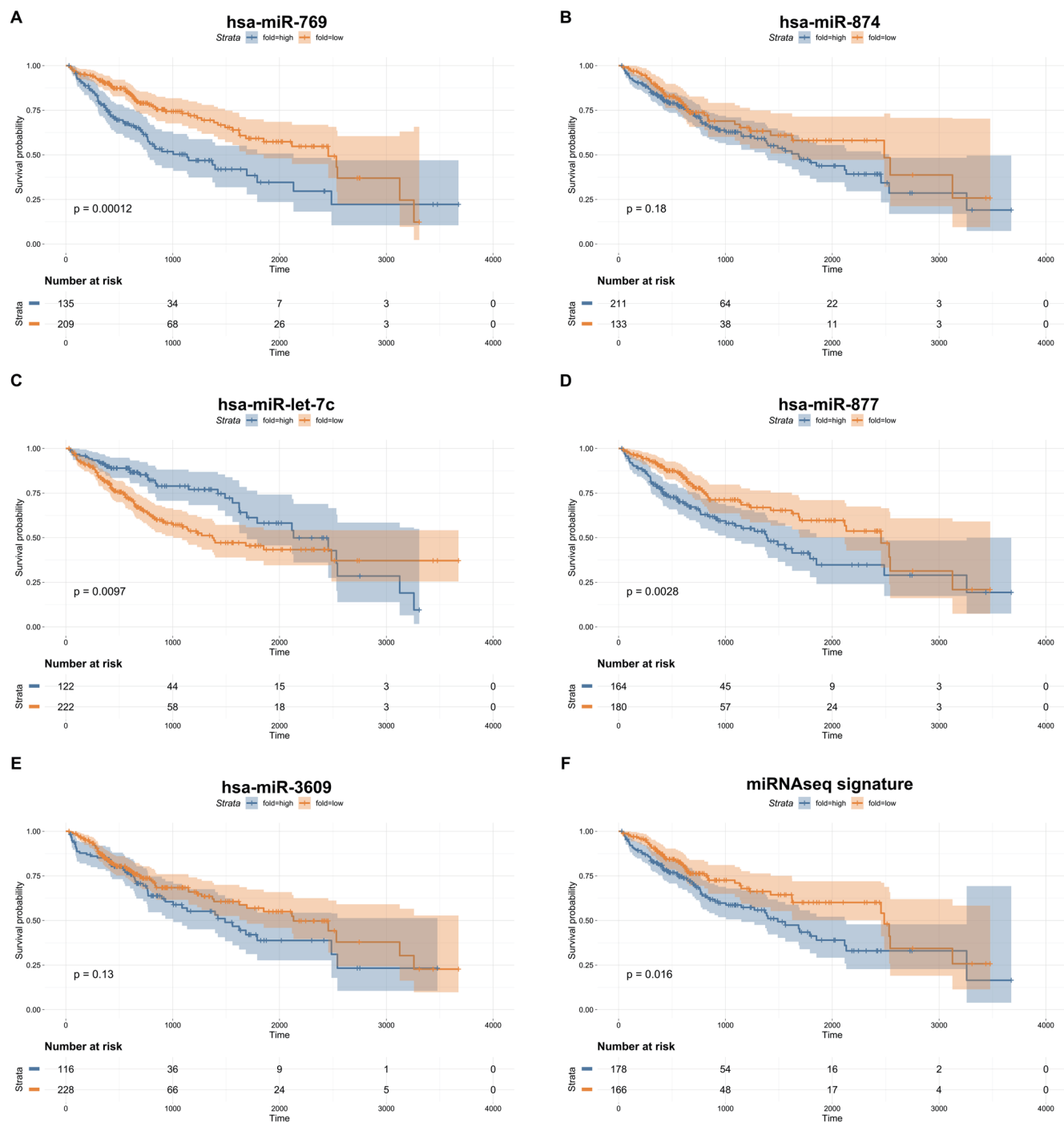
Fig. 5. Prognostic value of the miRNAseq signature in The Cancer Genome Atlas (TCGA) - Liver Hepatocellular Carcinoma (LIHC) patients. (A-F) Kaplan–Meier plots of miR-769 (A), miR-874 (B), miR-let-7c (C), miR-877 (D), miR-3609 (E) and the whole-signature (F) overall survival (OS) rates of patients in high expression (blue) and low expression (orange) groups stratified by *p*-value optimization of the miRNA signature.

depleted RNA pool sample and in the corresponding SCR control, both derived from the RNA samples employed for the high-throughput analyses. From the nanostring analysis, we validated miR-33a-5p and miR-378e, respectively down- and up-regulated upon APE1 depletion (Fig. 6A). From the RNAseq analysis (Fig. 6A) we validated miR-769, miR-let7-c, miR-877 (down-regulated upon APE1 depletion), and miR-3609 (up-regulated upon APE1 depletion).

Validation of JHH-6 DEmiRNAs in HCC tissue samples

A subset of validated DEmiRNAs, with expression consistent with the results obtained from the A549 and HeLa tumor cell lines,[13,16] was analyzed in HCC tissue samples with known APE1 protein levels in both tissue and matched serum. miR-
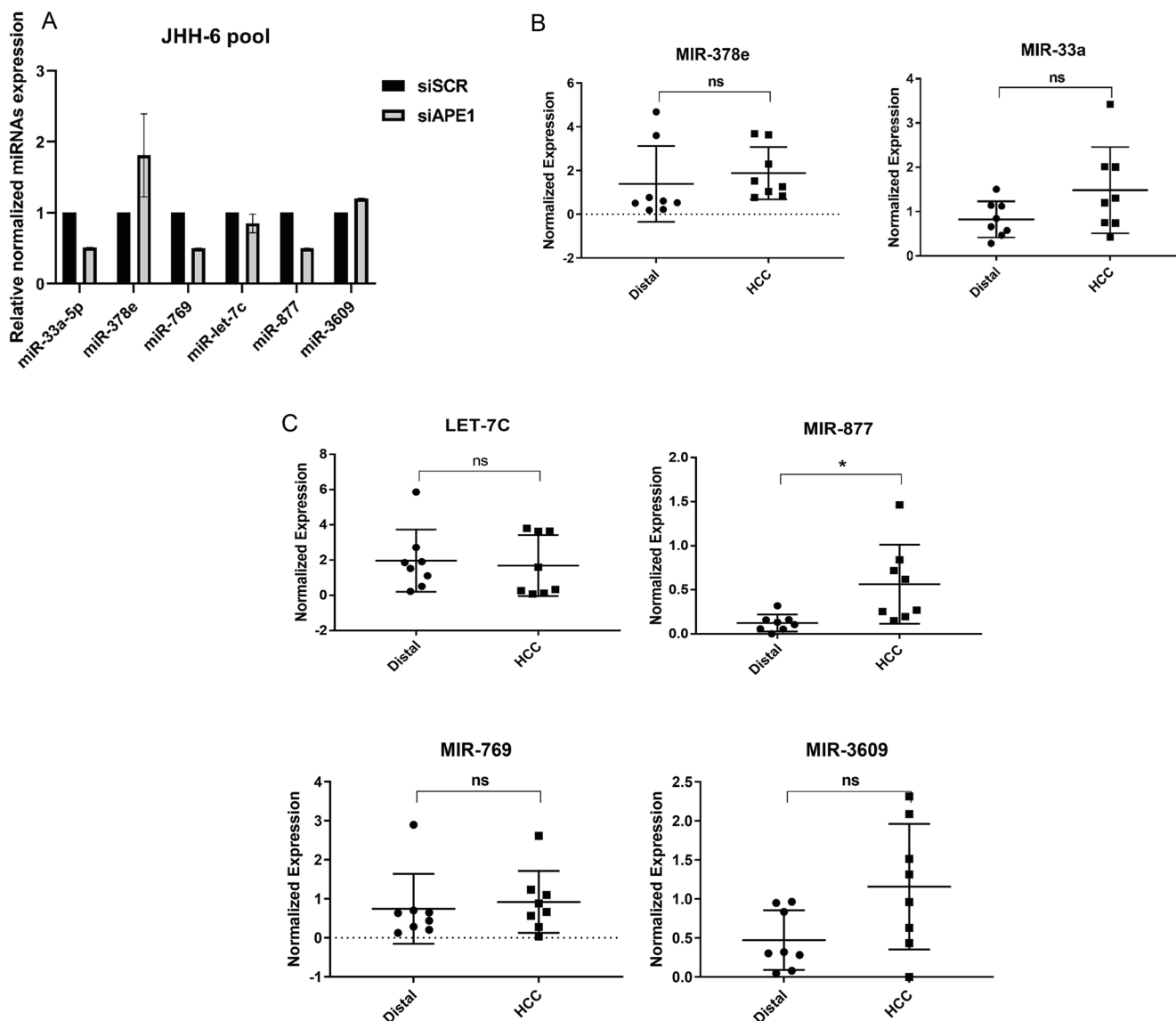
Fig. 6. Differentially-expressed microRNAs (DEmiRNAs) expression analysis in hepatocellular carcinoma (HCC) cells and tissue samples. (A) Quantitative real-time PCR (qRT-PCR) analysis performed in pooled RNA samples of JHH-6 cells depleted of APE1 and its respective pooled small interfering RNA (siRNA) scramble (siSCR) control to detection of DEmiRNA derived from nanostring and RNAseq analyses. (B) qRT-PCR analysis performed in RNA samples derived from HCC tissue samples (HCC) and their respective distal tissues (Distal) as control for the detection of DEmiRNA derived from nanostring analysis. (C) qRT-PCR analysis performed in RNA samples derived from HCC tissue samples (HCC) and their respective distal control tissues (Distal) for the detection of DEmiRNA derived from RNAseq analysis. Data are means±standard error of the means, *$p<0.05$.

378e and miR-33a-5p, derived from the nanostring analysis (Fig. 6B), and miR-let-7c, miR-877, miR-769, and miR-3609, derived from the RNAseq analysis, were assessed in eight HCC tissue samples and their respective distal nontumoral tissue (Fig. 6C). Unfortunately, only miR-877 was significantly overexpressed in HCC tissue samples compared with the relative controls (Fig. 6C).

Combined functional characterization of A549 and JHH-6 DEmiRNAs

To investigate if APE1 regulates a gene signature through miRNAs that could act on multiple cell/tissue types, we compared the list of TarBase/DIANA-MirPath[26] validated targets, obtained from the A549 nanostring experiment in our previous

work,[16] with the list derived from JHH-6. The Venn diagram shown in Figure 7A illustrates the overlap between the lists of validated targets regulated by A549 DEmiRNAs (*n*=3,814), JHH-6 DEmiRNAs (*n*=505), and by the two commonly regulated (miR-1246 and miR-33a-5p, *n*=864) DEmiRNAs. Taken together, these results suggest that approximately 20% of APE1-regulated miRNA targets in JHH-6 cells were specific to this cell line and were not affected in A549 cells (Fig. 7A). To investigate further, we focused specifically on nanostring targets that were differentially expressed in the corresponding dataset [abs(logFC) ≥1.0, adjusted $p≤0.05$)]. We looked at target genes that were expressed with inverse correlation to the identified miRNAs, identifying 18 transcripts expressed in JHH-6 cells (Supplementary Table 4) and 74 transcripts
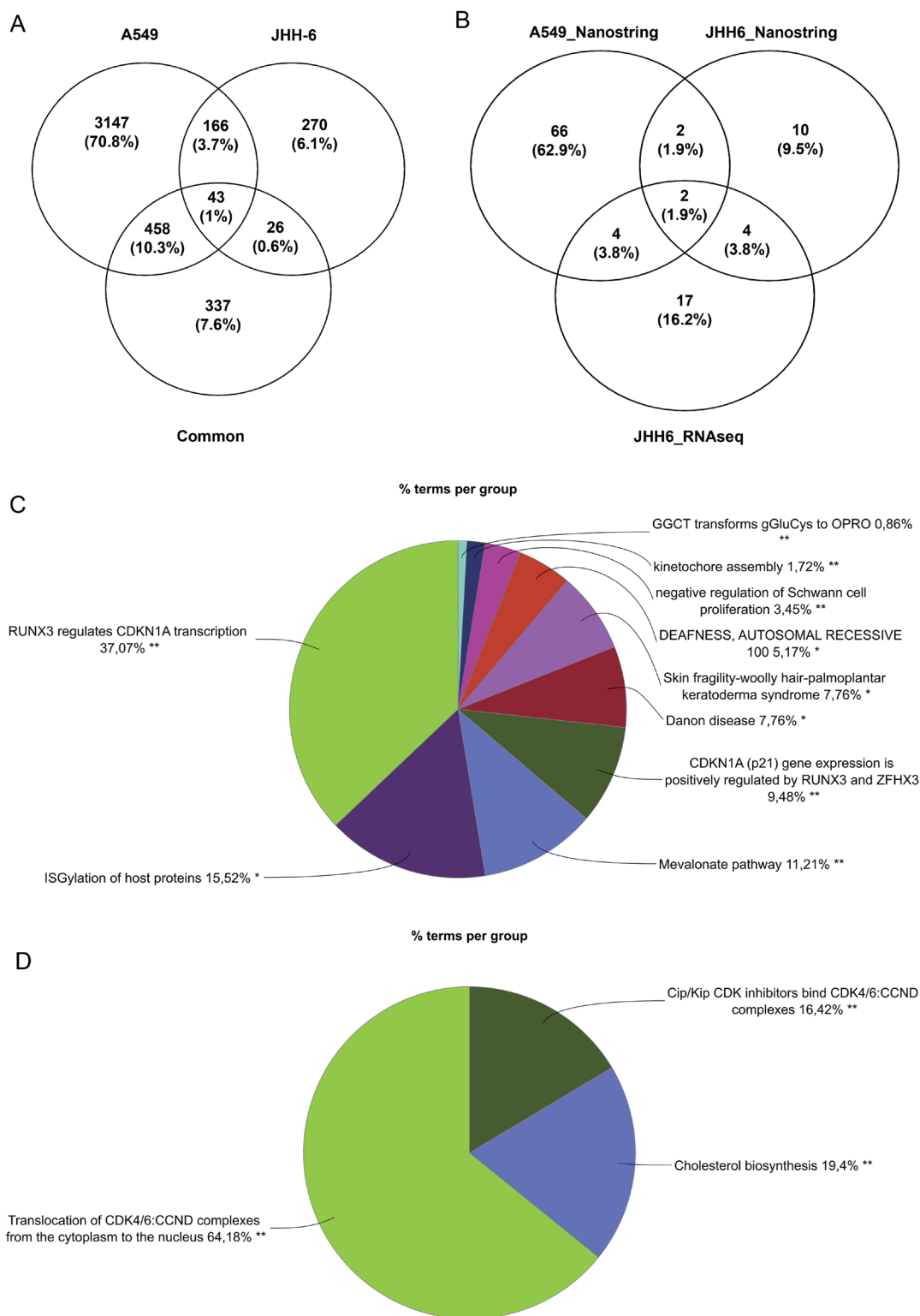
Fig. 7. Apurinic/apyrimidinic endodeoxyribonuclease 1 (APE1) regulates a gene signature through miRNAs that act on multiple cell/tissue types. (A) Venn diagram of the number of target genes regulated by nanostring-derived differentially-expressed microRNAs (DEmiRNAs) in A549 and JHH-6 cells. Common indicates the target genes of miR-1246 and miR-33a-5p that are differentially expressed in both cell lines. (B) Venn diagram of the number target genes coherently differentially expressed by their regulatory DEmiRNAs, as defined by nanostring analyses performed in A549 and JHH-6 cells and by RNAseq in JHH-6. (C) Pie chart of functional enrichment analysis results obtained for the JHH-6 differentially expressed target genes. (D) Pie chart of the common enriched functional terms associated with JHH-6 and A549 differentially expressed target genes.

expressed in A549 (Supplementary Table 5) that might represent the best candidate effectors of the examined phenotypes. By comparing the two sets of genes, we defined four common targets that were regulated in both cell lines: *CDK6*, *CREBL2*, *MBNL1*, and *SCML1*. Interestingly, these genes have a role in cell cycle regulation and mRNA splicing. We repeated the analysis including the JHH-6 RNAseq validated targets (Supplementary Table 6). The Venn diagram in Figure 7B shows that only two genes, *CDK6* and *SCML1,* were differentially expressed coherently with their regulating miRNAs in all three experiments. These genes are involved in cell cycle and transcription regulation. However, considering both miRNA expression profiling experiments that were performed in JHH-6 cells, this number increased to six common genes: *ANKRD52, LAMP2, PANK3, ZFHX3, CDK6,* and *SCML1*, which regulate transcription, cell cycle, and microvascular invasion.

Functional enrichment analyses of JHH-6 differentially expressed targets

Subsequently, we performed a pathway enrichment analysis of the differentially expressed targets in JHH-6 cells (n=18; Supplementary Table 4). As reported in Figure 7C, we found that APE1-regulated miRNAs impacted on biological processes involved in cancer progression, such as the Runt-related transcription factor 3 (RUNX3)-dependent regulation of Cyclin Dependent Kinase Inhibitor 1A (CDKN1A) transcription, mevalonate/cholesterol metabolism, ISGylation, Danon disease/LAMP2, Inositol hexakisphosphate (IP6)/inositol pentakisphosphate (IP5). We repeated the analysis with A549 cells (data not shown). In Figure 7D we show the two common terms identified in both functional enrichment analyses, Cyclin Dependent Kinase 4/Cyclin D1 and cholesterol metabolism, which have a major role in regulating tumor biological processes.[36,37]

Validation of APE1-regulated DEmiRNA targets and their expression in HCC

To elucidate the role of the putative effectors of the APE1-miRNA axis in HCC, we profiled the gene expression of the aforementioned DEmiRNAs validated targets (*CDK6, CREBL2, MBNL1, SCML1, ANKRD52, LAMP2, PANK3,* and *ZFHX3*) in the TCGA-LIHC/Genotype-Tissue Expression (commonly known as GTEx) datasets. All the examined targets were significantly up-regulated in HCC, except for *SCML1* which was down-regulated, although the difference with normal samples was not statistically significant (Fig. 8A). Subsequently, we conducted *in vitro* validation analysis of APE1-regulated miRNA targets using qRT-PCR. To do this, we used RNA pools of depleted APE1 and its related SCR control obtained from JHH-6 samples previously used for the high-throughput analyses. We chose to test two significantly up-regulated targets in HCC whose regulation is mediated by miR-33a-5p, an miRNA that is significantly regulated by APE1 in all cell lines tested so far:[13,16] *CDK6*, promoting G1/S transition and cell proliferation,[38] and *LAMP2*, which is involved in tumor progression and chemoresistance processes.[39] In Figure 8B, the histograms show that the down-regulation of APE1 induced the consequent up-regulation of these two DEmiRNA validated targets.

Validation of DEmiRNAs and their relative targets in hepatic and nonhepatic human cancer cell lines

To verify whether the identified DEmiRNAs could be also regulated by APE1 in other hepatic and nonhepatic human cell models, we analyzed their expression upon APE1 knockdown. For this purpose, we carried out APE1 silenc-

ing in Huh7 differentiated hepatocytes derived from cellular carcinoma, HepG2 well-differentiated hepatocarcinoma, A549 lung adenocarcinoma, HeLa cervical carcinoma, and HCT-116 colon carcinoma cell lines and analyzed the DEmiRNAs expression upon APE1 depletion using the specific siRNA sequence used above or using siRNA SCR as a control. The expression levels of the identified JHH-6 DEmiRNAs in all cell lines tested are shown in Figure 9A. In Huh7 cells, the JHH-6 DEmiRNAs were not significantly dysregulated upon APE1 silencing, while in HepG2 cells miR-33a-5p, miR-378e, miR-3609, and miR-1246 resulted significantly dysregulated. In A549 cells, we found miR-33a-5p and miR-1246 significantly dysregulated, as already reported in.[16] In HeLa cells, only three miRNAs (miR-877, miR-let-7c, and miR-1246) showed significant dysregulation. Similarly in HCT-116 cells, miR-769, miR-let7c, and miR-877 were dysregulated. Interestingly, in both cell lines, miR-let-7c showed an opposite trend compared with JHH-6 cells (Fig. 9A, B). The findings suggest that there are some common features of miRNA dysregulation across different cell lines, while some other are specific for each cell line.

We also investigated whether knocking down APE1 could impact the expression of DEmiRNA target genes in different cell lines. For this purpose, we performed gene expression analysis of *CDK6* and *LAMP2*, two targets of miR-33a-5p. As shown in Figure 9C, APE1 depletion in A549 and HeLa cell lines was associated with increased expression of *CDK6* and *LAMP2*, in accordance with a significant down-regulation of miR-33a-5p, similarly to JHH-6 cells. In HepG2 cells, *CDK6* resulted down-regulated, coherently with the significant up-regulation of miR-33a-5p. In HCT-116 cells, APE1-miRNA axis did not significantly affect any target gene, which is consistent with the nonsignificant dysregulation of miR-33a-5p. Finally, although no common DEmiRNAs were identified in Huh7, we observed a significant up-regulation of *CDK6* and *LAMP2* upon APE1 silencing. Thus, suggesting that APE1 could regulate these targets in Huh7 through different mechanisms. Overall, these findings support the role of the APE1-DEmiRNAs axis in the regulation of tumor progression and highlighting the importance of cell-specific mechanisms in this process.

Identification of circulating miRNAs correlating with sAPE1 levels in HCC patients

To identify miRNAs correlating with sAPE1 expression levels in HCC patients, we performed circulating miRNA microarray profiling in eight patients with high sAPE1 (126.58 pg/mL (85.42–161.92), median [95% confidence interval (CI)] vs. 10 patients with low median sAPE1 expression [(42.43 pg/mL (95% CI: 29.70–71.17), Supplementary Table 1]. Considering a FC cutoff of 2, we identified eight significant differentially expressed miRNAs (p<0.05) (Supplementary Table 7). miR-4492, miR-939, miR-3141, and miR-3180-3p positively correlated with sAPE1 levels, being higher in patients with high sAPE1 expression. Those miRNAs candidates were further investigated in the subsequent training phase.

Selection and validation of circulating miRNA candidates associated with sAPE1 levels

Considering our hypothesis regarding APE1's involvement in miRNA post-transcriptional processing, we selected miRNA candidates for the subsequent training and validation phases. Specifically, we focused on miRNAs that were down-regulated following APE1 silencing in cellular models, as well as miRNAs that were increased in the serum of patients with high sAPE1 levels (Supplementary Table 8). miRNA candi-
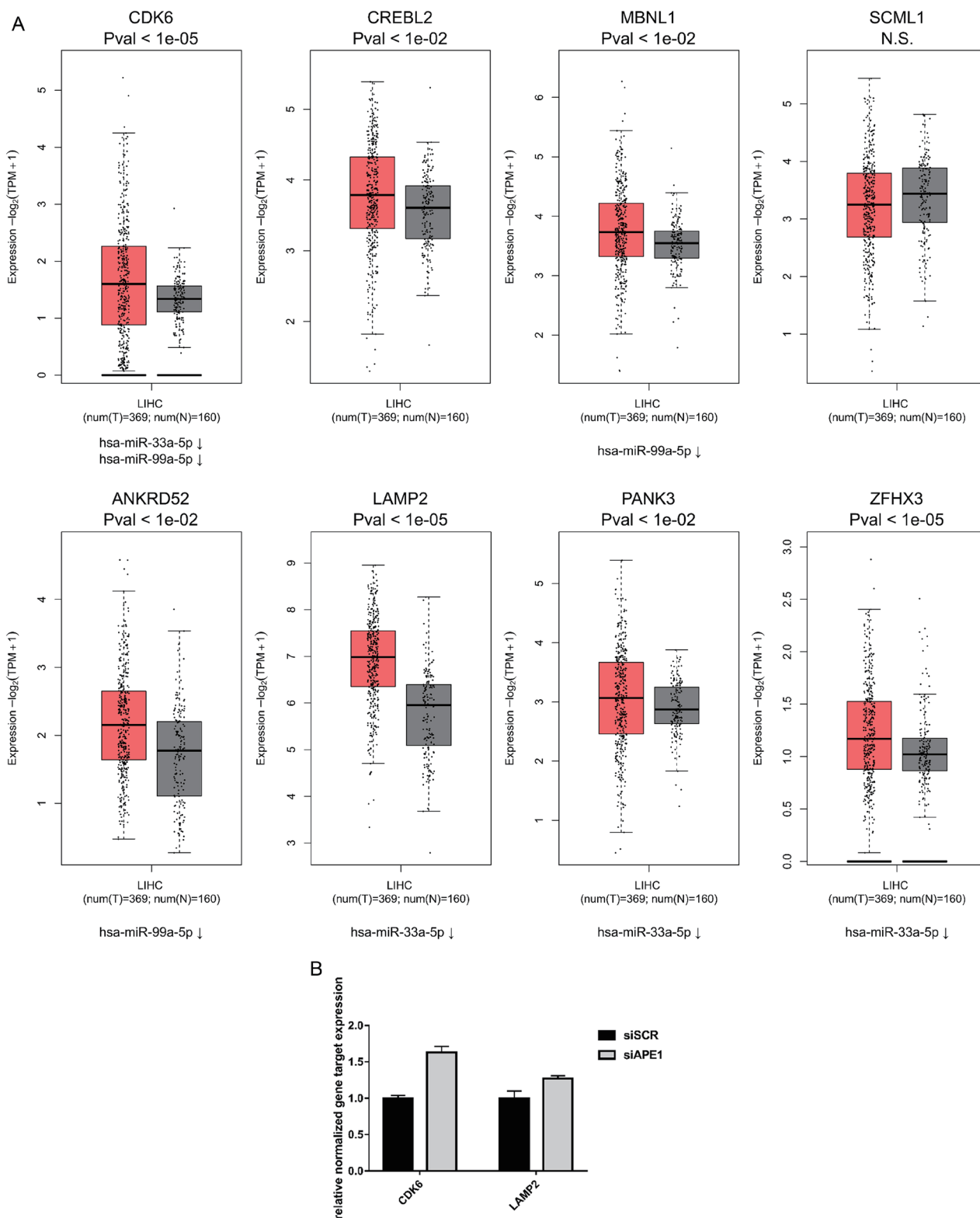
Fig. 8. Gene expression profiling of Differentially-expressed microRNAs (DEmiRNAs) validated targets in The Cancer Genome Atlas (TCGA) - Liver Hepatocellular Carcinoma (LIHC) dataset. (A) Boxplots of log2-transformed gene expression levels in the TCGA-LIHC (*n*=369) compared with the matched TCGA normal and Genotype-Tissue Expression (GTEx) datasets (*n*=160). Red: tumor; black: normal. The significance of every comparison is indicated on top of each plot. siAPE1 DEmiRNAs regulating each target are indicated below each plot (i.e. upon APE1 overexpression). (B) qRT-PCR analysis of CDK6 and LAMP2 mRNA expression in JHH-6 transiently depleted for APE1 pool and its respective SCR control pool. Histograms show data obtained by the ΔΔCT method with GAPDH, actin, and 28S as reference genes.
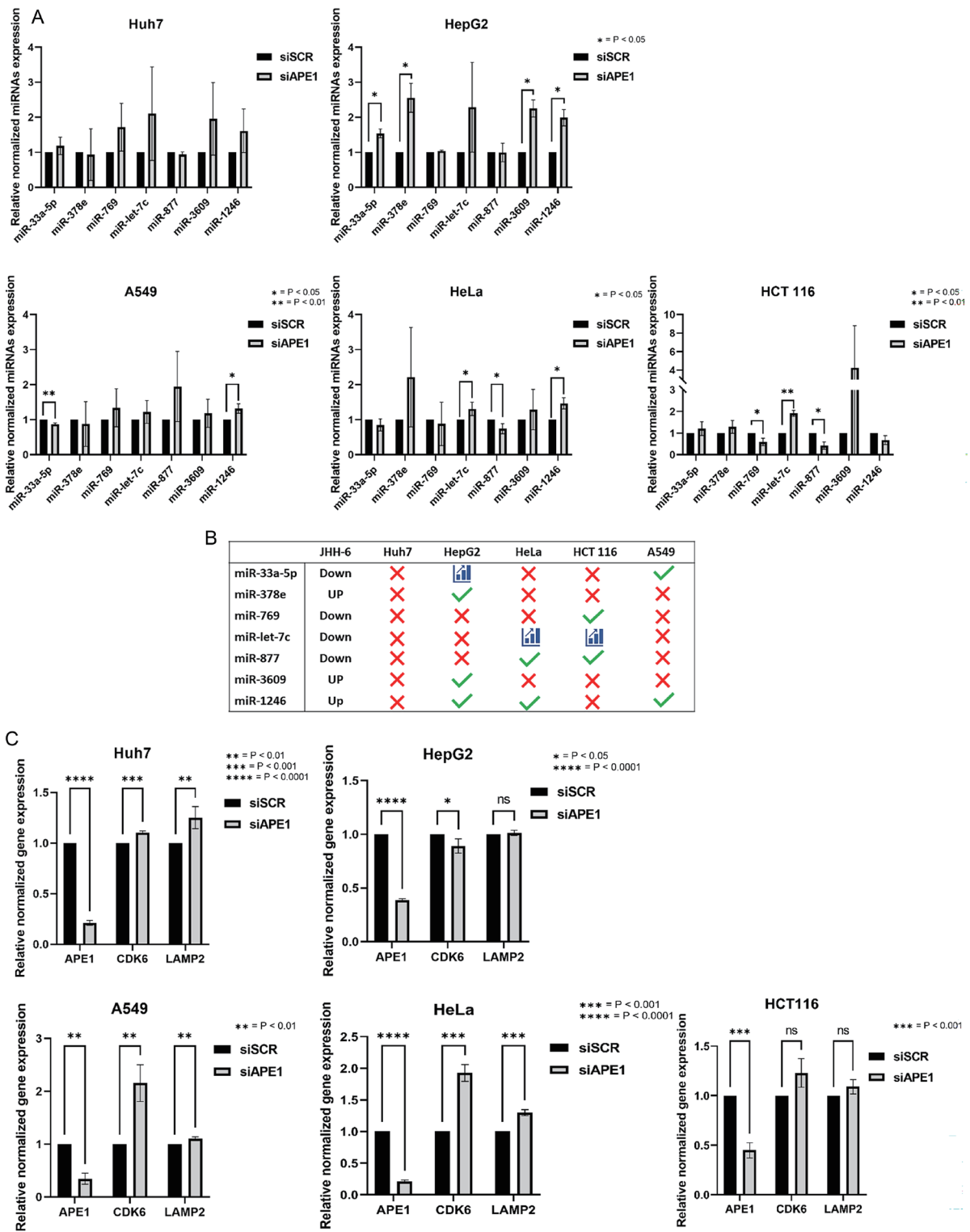
Fig. 9. Differentially-expressed microRNAs (DEmiRNAs) and target gene expression analysis in hepatic and nonhepatic cell lines. (A) Quantitative real-time PCR (qRT-PCR) analysis for the detection of DEmiRNAs derived from nanostring and RNAseq analyses were performed in RNA samples derived from Huh7, HepG2, A549, HeLa, and HCT-116 cells in the condition of APE1-depletion and in its respective small interfering RNA (siRNA) scramble (siSCR)-treated control. (B) Graph summarizing significant (green), nonsignificant (red) and significant with opposite trend (blue) miRNAs, derived from expression analysis performed in Huh7, HepG2, A549, HeLa, and HCT-116 cells to validate JHH-6 DE-miRNAs indicated on the left. (C) qRT-PCR analysis of APE1, CDK6, and LAMP2 mRNA expression in Huh7, HepG2, A549, HeLa, and HCT-116 cells, transiently depleted for APE1 and their respective SCR controls. Histograms show data obtained by the ΔΔCT method with 28S as the reference gene. Data are means±SD of three independent replicates, *p<0.05, **p<0.01, ***p<0.001, ****p<0.0001.

dates were analyzed by qRT-PCR in the serum of 24 patients with HCC (Supplementary Table 1), Twelve of them had high sAPE1 expression and 12 had low sAPE1 expression. The median sAPE1 expression was 161.48 pg/mL (95% CI: 141.48–208.19) in the high expression group and 32.31 pg/mL (95% CI: 18.97–40.35) in the low expression group, p0.001.

Despite some trends being visible in the correlation between sAPE1 and circulating miRNAs, only miR-769 and miR-3180-3p showed a significant correlation (p=0.046, Pearson correlation 0.45, p=0.047, Pearson correlation 0.42, respectively; Fig. 10A). Among the miRNA candidates listed in Supplementary Table 8, we were unable to replicate the miR-3141 results observed in the miRNA microarray. That was because of the high GC content of the miRNA sequence, which led to multiple unspecific amplifications during qRT-PCR. The correlation between circulating miR-3180-3p and miR-769 with sAPE1 was further assessed in 67 samples obtained from HCC patients (Supplementary Table 1). Despite the initial correlation evidenced during the training phase, neither miR-769 nor miR-3180-3p were correlated with sAPE1 levels when validated in a larger group of patients (Fig. 10B, C).

Discussion

HCC is one of the most fatal cancer types worldwide.[1] The absence of tools for an accurate early diagnose the disease, stratify patients, and predict prognosis negatively impacts patient survival. In the last few years, great efforts were dedicated to the discovery of reliable biomarkers fulfilling all these unmet clinical needs. Our previous research confirmed that sAPE1 has the potential to serve as a reliable biomarker for distinguishing patients with HCC from patients with cirrhosis.[21] APE1 is highly expressed in HCC where, besides its involvement in the base excision repair process, it may participate in many other cancer-related pathways.[12] Indeed, high APE1 tissue levels have been associated with unfavorable prognosis in cancer patients, and data from TC-GA-LIHC confirmed the same trend for HCC patients. APE1 has been found to participate in the maturation of certain cellular miRNAs, as recently discovered. However, it remains unclear whether this process is associated with cancer and which specific miRNAs are involved.[13] Thus, this observation opened new intriguing aspects in the role of APE1 in cancer, especially in relation to those miRNAs that are released in biofluids.

In this study, we found an alteration of the cellular miRNA expression profile upon APE1 depletion. In JHH-6 cancer cells, the changes involved several miRNAs (miR-let7c-5p, miR-33a-5p, miR-99a-5p, miR-378e, miR-575, miR-769, miR-874, miR-877, miR-1246, miR-1973, miR-2117, miR-3609, and miR-6087) participating in metabolic and signaling pathways related to cell proliferation (*PI3K/AKT* pathway[32] and choline metabolism[33]), transformation (*ERBB* signaling[34]), angiogenesis, and RNA maturation. Interestingly, higher amounts of miR-99a-5p or miR-let7c-5p and lower levels of miR-33a-5p, miR-769, or miR-877, were associated with a better outcome in TCGA patients. Thus, the evidence on miR-33a-5p, miR-769, and miR-877 support the hypothesis of a possible involvement of APE1 in the regulation of oncomiRs. Indeed, higher tumor tissue levels of miR-33a-5p, miR-769, miR-877, and APE1 correlate with a worse prognosis for the patient. In agreement with these data, we observed an up-regulation of miR-33a-5p and miR-877 in tumor tissue compared with the distal portion of the liver, even if only miR-877 was statistically significant. The results of our study are consistent with our previous findings that sAPE1

protein levels are significantly elevated in HCC compared with both cirrhosis and healthy blood donors. Moreover, in HCC tissue the levels of APE1 mRNA and protein were higher compared to surrounding liver cirrhosis, peri-HCC, or healthy control tissues, in accordance with sAPE1 levels.[21] It is worth noticing that, among the validated DEmiRNAs we found, only miR-769 was consistent with literature reports.[40] However, conflicting data regarding miR-33a-5p[41,42] and miR-877[43] and their prognostic value in HCC exist, highlighting the need for further investigation. Functional enrichment analysis of JHH-6 DEmiRNA differentially expressed targets suggested a role in biological processes involved in cancer progression, such as the RUNX3-dependent regulation of CDKN1A transcription, mevalonate/cholesterol metabolism, ISGylation, Danon disease/LAMP2, IP5/IP6. The relevance of these biological processes in cancer is evident, indeed: IP6 represses cell growth and promotes cell differentiation,[44] while ISGylation promotes the genesis and progression of malignancies and regulates exosome secretion.[45]

Interestingly, the mevalonate pathway offers several potential targets for cancer therapy in HCC.[46] However, contrasting information about LAMP2 expression and its role in HCC exists. Indeed, low LAMP2 expression seems to be correlated with microvascular invasion and poor prognosis in HCC,[47] while other studies demonstrated that increased stability of the protein mediated by the long noncoding RNA FAM215A, induces doxorubicin resistance and tumor progression.[39] Altogether this evidence suggests that APE1 may sustain HCC tumor progression through miRNAs regulation.

To further investigate the potential role of those DEmiRNAs as biomarkers, we profiled the serum of HCC patients. It is well known that miRNAs represent the most promising class of circulating biomarkers, by virtue of their stability in biofluids, easy detectability and, last but not least, their fundamental role in the disease.[48] Thus, tumors expressing high levels of APE1 may release larger quantities of APE1-regulated miRNAs, which may help in stratifying patients and predicting their prognosis. Assuming that patients with overexpressed APE1 in tissue may have augmented APE1 levels in biofluids,[13,16,20,21] we investigated the association of circulating miRNAs with sAPE1 levels. By comparing patients expressing high levels of sAPE1 to patients with low sAPE1, we identified eight miRNAs differently expressed between the two groups. Interestingly, none of these miRNAs were dysregulated upon APE1 depletion in our cell model, suggesting an indirect association with sAPE1 levels in biofluids. miRNAs positively associated with higher sAPE1 levels, miR-939, miR-3141, miR-3180-3p, and miR-4492, were assessed in serum samples from HCC patients. Although the training phase identified miR-3180-3p as a possible circulating miRNA positively correlated with sAPE1 levels, the subsequent validation phase evidenced no association between the miRNA and sAPE1. The limited information available in the literature about miR-3180-3p limits the speculations about our observation. Nevertheless, miR-3180-3p was reported to downregulate regulatory factor X1 (also referred to as *RFX1*),[49] which has both anticancer and cancer-promoting activities.[50] Indeed, it can regulate the expression of several proto-oncogenes as well as tumor suppressors, depending on tumor type and on spatial and temporal expression.[50] Thus, the interpretation of our results still needs more evidence about the role of this miRNA in cancer. The serum levels of three miRNAs, which demonstrated a consistent down-regulation upon APE1 silencing in cells and exhibited negative prognostic value in the TCGA cohort, were evaluated in HCC patients, yielding similar results. Although an initial analysis showed a significant correlation (Pearson correlation 0.45, p=0.046)
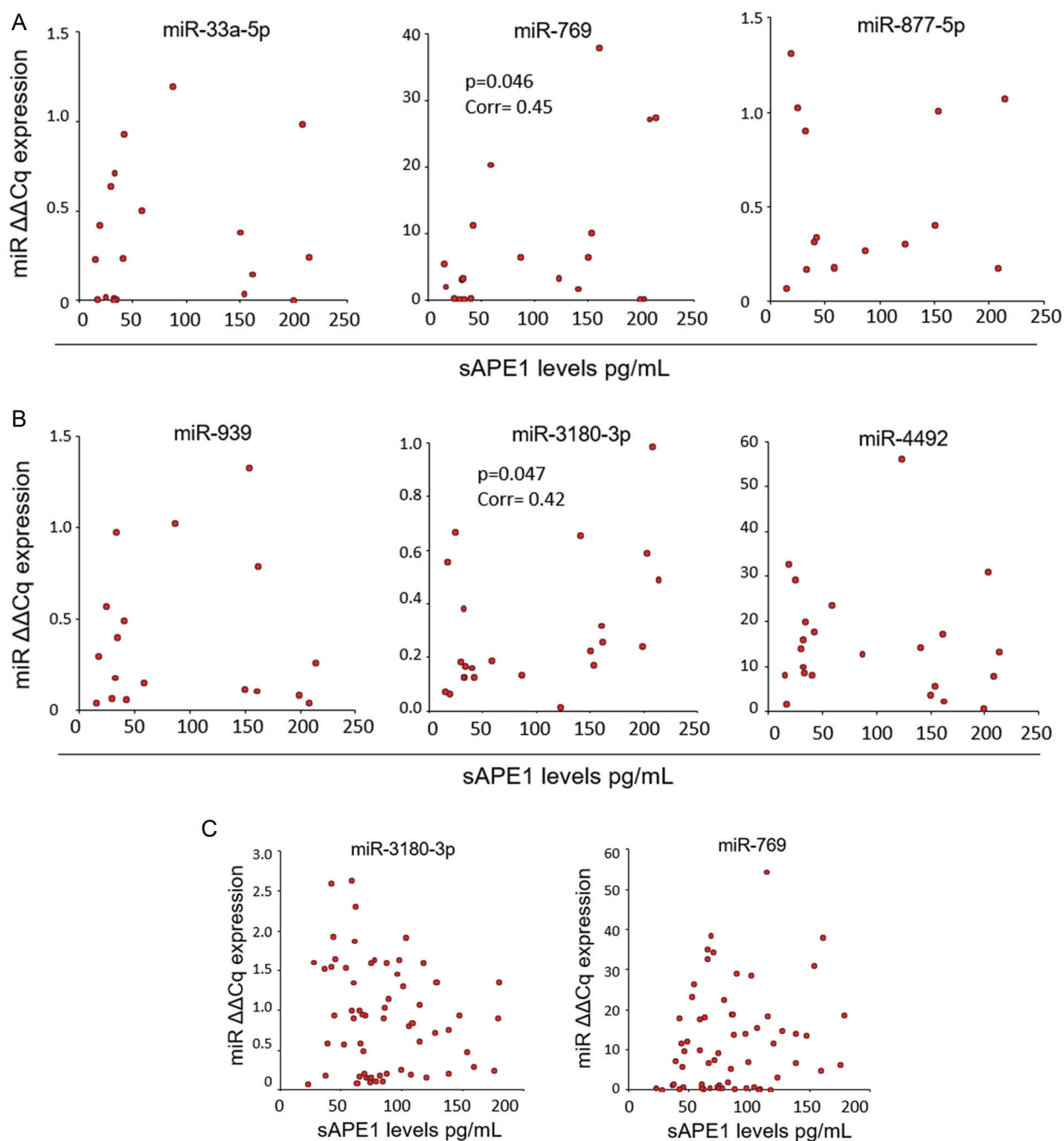
Fig. 10. Correlation charts of circulating miRNAs and sAPE1 in patients with HCC. (A) miRNA and sAPE1 Pearson correlation in serum of hepatocellular carcinoma (HCC) patients. Expression of the selected miRNA candidates was correlated with the expression of serum APE1 (sAPE1) and normalized against serum miR-1280 and miR-1275. (B) sAPE1 expression in HCC patients selected for the validation phase. sAPE1 levels were expressed in pg/mL. *p*-values were computed by the nonparametric Mann-Whitney U in *a t*-test procedures. (C) miR-3180-3p and sAPE1 Pearson correlation in serum from HCC patients. The expression of miR-3180-3p was correlated with the expression of sAPE1 in 67 HCC patients normalized against serum miR-1280 and miR-1275.

between miR-769 and sAPE1 levels, further validation in the serum of HCC patients did not yield the expected results (Pearson correlation 0.2, *p*=0.12). Despite proof of miR-769 being involved in cell proliferation, invasion, and poor OS in HCC,[40] the clinical meaning of its presence in serum is still unclear. Evidence from other cancers[51,52] has shown that this miRNA is present in exosomes released by cancer cells. Therefore, focusing on the serum exosomal fraction alone could aid in interpreting the cancer-related information conveyed by miR-769. Other study limitations are: (1) a small sample size, with results that should ideally be validated in a much larger study population; (2) incomplete information associated with miRNA expression in the databases used for the analysis; and (3) lack of knowledge of the biological function of some miRNA candidates in HCC that would strengthen their role as biomarkers.

Conclusions

In this study, we investigated whether novel miRNAs regulated by APE1 participated in liver oncogenesis and served as prognostic biomarkers. In our cellular models, we found that APE1 silencing led to changes in the expression of certain miRNAs, including miR-877, which showed increased expression in HCC tumor samples and was negatively associated with patient OS. Together with our previous results, the observations suggest an important role of APE1 in the processing of specific miRNAs involved in several cellular pathways, some of which are considered hallmarks of cancer. However, we were unable to find consistent data when analyzing serum samples, possibly owing to confounding factors present in biofluids. This problem could be solved by using new techniques and/or technologies able to specifically isolate liver-derived exosomes, thus boosting the research on biomarkers for liver diseases. Indeed, the lack of reliable biomarkers and predictive models result in poor patient outcomes, especially in HCC. In fact, HCC remains one of the deadliest cancers worldwide and the need for new tools to clinicians stratify patients is of utmost priority in clinical oncology.

Funding

Conflict of interest

CT has been an editorial board member of *Journal of Clinical and Translational Hepatology* since 2013. The other authors have no conflict of interests related to this publication.

Author contributions

Designed and conceived the study and supervised the experiments (GT, CT), designed and performed most of the experiments, analyzed the data and critically contributed to the interpretation of the results (GM, DP), performed the bioinformatics analysis (ED), performed the NGS sequencing (VDS), performed the NGS bioinformatic analysis (SP, GC), collected clinical samples (LSC), contributed validation experiments (GA, MDG), and performed the bulk of the writing of the manuscript (GM, DP, CT, GT). All authors critically read and approved the final version of the manuscript.

Ethical statement

Written informed consent was provided by all patients. Investigation was conducted following the principles in the Declaration of Helsinki. The study was approved by the regional ethical committee (Comitato Etico Regionale Unico FVG, No. 14/2012 ASUITS and Prot. No. 2018 Os-008-ASUITS, CINE-CA No. 2225).

Data sharing statement

Data used to support the findings of this study have been deposited in [GEO] superseries: GSE222853. For nanostring data: GSE222851. For RNAseq data: GSE222852. To review GEO accession GSE222853: go to https://www.ncbi.nlm.nih.gov/geo/query/acc.cgi?acc=GSE222853 and enter token qloxyasshfgxzev into the box.

References

[1] Llovet JM, Kelley RK, Villanueva A, Singal AG, Pikarsky E, Roayaie S, *et al*. Hepatocellular carcinoma. Nat Rev Dis Primers 2021;7(1):6. doi:10.1038/s41572-020-00240-3, PMID:33479224.

[2] European Association for the Study of the Liver. EASL Clinical Practice Guidelines: Management of hepatocellular carcinoma. J Hepatol 2018;69(1):182–236. doi:10.1016/j.jhep.2018.03.019, PMID:29628281.

[3] Marrero JA, Kulik LM, Sirlin CB, Zhu AX, Finn RS, Abecassis MM, *et al*. Diagnosis, Staging, and Management of Hepatocellular Carcinoma: 2018 Practice Guidance by the American Association for the Study of Liver Diseases. Hepatology 2018;68(2):723–750. doi:10.1002/hep.29913, PMID:29624699.

[4] Schulze K, Imbeaud S, Letouzé E, Alexandrov LB, Calderaro J, Rebouissou S, *et al*. Exome sequencing of hepatocellular carcinomas identifies new mutational signatures and potential therapeutic targets. Nat Genet 2015;47(5):505–511. doi:10.1038/ng.3252, PMID:25822088.

[5] Zucman-Rossi J, Villanueva A, Nault JC, Llovet JM. Genetic Landscape and Biomarkers of Hepatocellular Carcinoma. Gastroenterology 2015;149(5):1226–1239.e4.doi:10.1053/j.gastro.2015.05.061,PMID:26099527.

[6] Yang SF, Chang CW, Wei RJ, Shiue YL, Wang SN, Yeh YT. Involvement of DNA damage response pathways in hepatocellular carcinoma. Biomed Res Int 2014;2014:153867. doi:10.1155/2014/153867, PMID:24877058.

[7] Chen CC, Chen CY, Ueng SH, Hsueh C, Yeh CT, Ho JY, *et al*. Corylin increases the sensitivity of hepatocellular carcinoma cells to chemotherapy through long noncoding RNA RAD51-AS1-mediated inhibition of DNA repair. Cell Death Dis 2018;9(5):543. doi:10.1038/s41419-018-0575-0, PMID:29749376.

[8] Al-Hrout A, Chaiboonchoe A, Khraiwesh B, Murali C, Baig B, El-Awady R, *et al*. Safranal induces DNA double-strand breakage and ER-stress-mediated cell death in hepatocellular carcinoma cells. Sci Rep 2018;8(1):16951. doi:10.1038/s41598-018-34855-0, PMID:30446676.

[9] Jobert L, Nilsen H. Regulatory mechanisms of RNA function: emerging roles of DNA repair enzymes. Cell Mol Life Sci 2014;71(13):2451–2465. doi:10.1007/s00018-014-1562-y, PMID:24496644.

[10] Tell G, Demple B. Base excision DNA repair and cancer. Oncotarget 2015;6(2):584–585. doi:10.18632/oncotarget.2705, PMID:25655644.

[11] Kim WC, King D, Lee CH. RNA-cleaving properties of human apurinic/apyrimidinic endonuclease 1 (APE1). Int J Biochem Mol Biol 2010;1(1):12–25. PMID:21968700.

[12] Tell G, Quadrifoglio F, Tiribelli C, Kelley MR. The many functions of APE1/Ref-1: not only a DNA repair enzyme. Antioxid Redox Signal 2009;11(3):601–620. doi:10.1089/ars.2008.2194, PMID:18976116.

[13] Antoniali G, Serra F, Lirussi L, Tanaka M, D'Ambrosio C, Zhang S, *et al*. Mammalian APE1 controls miRNA processing and its interactome is linked to cancer RNA metabolism. Nat Commun 2017;8(1):797. doi:10.1038/s41467-017-00842-8, PMID:28986522.

[14] Ayyildiz D, Antoniali G, D'Ambrosio C, Mangiapane G, Dalla E, Scaloni A, *et al*. Architecture of The Human Ape1 Interactome Defines Novel Cancers Signatures. Sci Rep 2020;10(1):28. doi:10.1038/s41598-019-56981-z, PMID:31913336.

[15] Dai N, Zhong ZY, Cun YP, Qing Y, Chen Ch, Jiang P, *et al*. Alteration of the microRNA expression profile in human osteosarcoma cells transfected with APE1 siRNA. Neoplasma 2013;60(4):384–394. doi:10.4149/neo_2013_050, PMID:23581410.

[16] Antoniali G, Dalla E, Mangiapane G, Zhao X, Jing X, Cheng Y, *et al*. APE1 controls DICER1 expression in NSCLC through miR-33a and miR-130b. Cell Mol Life Sci 2022;79(8):446. doi:10.1007/s00018-022-04443-7, PMID:35876890.

[17] Yang F, Ning Z, Ma L, Liu W, Shao C, Shu Y, *et al*. Exosomal miRNAs and miRNA dysregulation in cancer-associated fibroblasts. Mol Cancer 2017;16(1):148. doi:10.1186/s12943-017-0718-4, PMID:28851377.

[18] Shin JH, Choi S, Lee YR, Park MS, Na YG, Irani K, *et al*. APE1/Ref-1 as a Serological Biomarker for the Detection of Bladder Cancer. Cancer Res Treat 2015;47(4):823–833. doi:10.4143/crt.2014.074, PMID:25672588.

[19] Wei X, Li YB, Li Y, Lin BC, Shen XM, Cui RL, *et al*. Prediction of Lymph Node Metastases in Gastric Cancer by Serum APE1 Expression. J Cancer 2017;8(8):1492–1497. doi:10.7150/jca.18615, PMID:28638465.

[20] Zhang S, He L, Dai N, Guan W, Shan J, Yang X, *et al*. Serum APE1 as a predictive marker for platinum-based chemotherapy of non-small cell lung cancer patients. Oncotarget 2016;7(47):77482–77494. doi:10.18632/oncotarget.13030, PMID:27813497.

[21] Pascut D, Sukowati CHC, Antoniali G, Mangiapane G, Burra S, Mascaretti LG, *et al*. Serum AP-endonuclease 1 (sAPE1) as novel biomarker for hepatocellular carcinoma. Oncotarget 2019;10(3):383–394. doi:10.18632/oncotarget.26555, PMID:30719231.

[22] Mangiapane G, Parolini I, Conte K, Malfatti MC, Corsi J, Sanchez M, *et al*. Enzymatically active apurinic/apyrimidinic endodeoxyribonuclease 1 is released by mammalian cells through exosomes. J Biol Chem 2021;296:100569. doi:10.1016/j.jbc.2021.100569, PMID:33753167.

[23] Fujise K, Nagamori S, Hasumura S, Homma S, Sujino H, Matsuura T, *et al*. Integration of hepatitis B virus DNA into cells of six established human hepatocellular carcinoma cell lines. Hepatogastroenterology 1990;37(5):457–460. PMID:1701409.

[24] Aden DP, Fogel A, Plotkin S, Damjanov I, Knowles BB. Controlled synthesis of HBsAg in a differentiated human liver carcinoma-derived cell line. Nature 1979;282(5739):615–616. doi:10.1038/282615a0, PMID:233137.

[25] Nakabayashi H, Taketa K, Miyano K, Yamane T, Sato J. Growth of human hepatoma cells lines with differentiated functions in chemically defined medium. Cancer Res 1982;42(9):3858–3863. PMID:6286115.

[26] Vlachos IS, Zagganas K, Paraskevopoulou MD, Georgakilas G, Karagkouni D, Vergoulis T, *et al*. DIANA-miRPath v3.0: deciphering microRNA function with experimental support. Nucleic Acids Res 2015;43(W1):W460–W466. doi:10.1093/nar/gkv403, PMID:25977294.

[27] Minadakis G, Zachariou M, Oulas A, Spyrou GM. PathwayConnector: finding complementary pathways to enhance functional analysis. Bioinformatics 2019;35(5):889–891. doi:10.1093/bioinformatics/bty693, PMID:30124768.

[28] Tang Z, Kang B, Li C, Chen T, Zhang Z. GEPIA2: an enhanced web server for large-scale expression profiling and interactive analysis. Nucleic Acids Res 2019;47(W1):W556–W560. doi:10.1093/nar/gkz430, PMID:31114875.

[29] European Association For The Study Of The Liver, European Organisation For Research And Treatment Of Cancer. EASL-EORTC clinical practice guidelines: management of hepatocellular carcinoma. J Hepatol 2012;56(4):908–943. doi:10.1016/j.jhep.2011.12.001, PMID:22424438.

[30] Pascut D, Krmac H, Gilardi F, Patti R, Calligaris R, Crocè LS, *et al*. A comparative characterization of the circulating miRNome in whole blood and serum of HCC patients. Sci Rep 2019;9(1):8265. doi:10.1038/s41598-019-44580-x, PMID:31164669.

[31] Cerami E, Gao J, Dogrusoz U, Gross BE, Sumer SO, Aksoy BA, *et al*. The cBio cancer genomics portal: an open platform for exploring multidimensional cancer genomics data. Cancer Discov 2012;2(5):401–404. doi:10.1158/2159-8290.CD-12-0095, PMID:22588877.

[32] Zhou Q, Lui VW, Yeo W. Targeting the PI3K/Akt/mTOR pathway in hepatocellular carcinoma. Future Oncol 2011;7(10):1149–1167. doi:10.2217/fon.11.95, PMID:21992728.

[33] Kuang Y, Salem N, Corn DJ, Erokwu B, Tian H, Wang F, *et al*. Transport and metabolism of radiolabeled choline in hepatocellular carcinoma. Mol Pharm 2010;7(6):2077–2092. doi:10.1021/mp1001922, PMID:20698576.

[34] Berasain C, Avila MA. The EGFR signalling system in the liver: from hepatoprotection to hepatocarcinogenesis. J Gastroenterol 2014;49(1):9–23. doi:10.1007/s00535-013-0907-x, PMID:24318021.

[35] Takino J, Yamagishi S, Takeuchi M. Glycer-AGEs-RAGE signaling enhances the angiogenic potential of hepatocellular carcinoma by upregulating VEGF expression. World J Gastroenterol 2012;18(15):1781–1788. doi:10.3748/wjg.v18.i15.1781, PMID:22553402.

[36] Xu H, Zhou S, Tang Q, Xia H, Bi F. Cholesterol metabolism: New functions and therapeutic approaches in cancer. Biochim Biophys Acta Rev Cancer 2020;1874(1):188394. doi:10.1016/j.bbcan.2020.188394, PMID:32698040.

[37] Gao X, Leone GW, Wang H. Cyclin D-CDK4/6 functions in cancer. Adv Cancer Res 2020;148:147–169. doi:10.1016/bs.acr.2020.02.002, PMID:32723562.

[38] Wang YL, Liu JY, Yang JE, Yu XM, Chen ZL, Chen YJ, *et al*. Lnc-UCID Promotes G1/S Transition and Hepatoma Growth by Preventing DHX9-Mediated CDK6 Down-regulation. Hepatology 2019;70(1):259–275. doi:10.1002/hep.30613, PMID:30865310.

[39] Huang PS, Lin YH, Chi HC, Tseng YH, Chen CY, Lin TK, *et al*. Dysregulated FAM215A Stimulates LAMP2 Expression to Confer Drug-Resistant and Malignant in Human Liver Cancer. Cells 2020;9(4):961. doi:10.3390/cells9040961, PMID:32295144.

[40] Xian Y, Wang L, Yao B, Yang W, Mo H, Zhang L, *et al*. MicroRNA-769-5p contributes to the proliferation, migration and invasion of hepatocellular carcinoma cells by attenuating RYBP. Biomed Pharmacother 2019;118:109343. doi:10.1016/j.biopha.2019.109343, PMID:31545279.

[41] Chang W, Zhang L, Xian Y, Yu Z. MicroRNA-33a promotes cell proliferation and inhibits apoptosis by targeting PPARα in human hepatocellular carcinoma. Exp Ther Med 2017;13(5):2507–2514. doi:10.3892/etm.2017.4236, PMID:28565872.

[42] Xie RT, Cong XL, Zhong XM, Luo P, Yang HQ, Lu GX, *et al*. MicroRNA-33a downregulation is associated with tumorigenesis and poor prognosis in patients with hepatocellular carcinoma. Oncol Lett 2018;15(4):4571–4577. doi:10.3892/ol.2018.7892, PMID:29541227.

[43] Huang X, Qin J, Lu S. Up-regulation of miR-877 induced by paclitaxel inhibits hepatocellular carcinoma cell proliferation though targeting FOXM1. Int J Clin Exp Pathol 2015;8(2):1515–1524. PMID:25973036.

[44] Vucenik I, Tantivejkul K, Zhang ZS, Cole KE, Saied I, Shamsuddin AM. IP6 in treatment of liver cancer. I. IP6 inhibits growth and reverses transformed phenotype in HepG2 human liver cancer cell line. Anticancer Res 1998;18(6A):4083–4090. PMID:9891449.

[45] Villarroya-Beltri C, Guerra S, Sánchez-Madrid F. ISGylation - a key to lock the cell gates for preventing the spread of threats. J Cell Sci 2017;130(18):2961–2969. doi:10.1242/jcs.205468, PMID:28842471.

[46] Ogura S, Yoshida Y, Kurahashi T, Egawa M, Furuta K, Kiso S, *et al*. Targeting the mevalonate pathway is a novel therapeutic approach to inhibit oncogenic FoxM1 transcription factor in human hepatocellular carcinoma. Oncotarget 2018;9(30):21022–21035. doi:10.18632/oncotarget.24781, PMID:29765517.

[47] Zheng H, Yang Y, Ye C, Li PP, Wang ZG, Xing H, *et al*. Lamp2 inhibits epithelial-mesenchymal transition by suppressing Snail expression in HCC. Oncotarget 2018;9(54):30240–30252. doi:10.18632/oncotarget.25367, PMID:30100986.

[48] Morishita A, Masaki T. miRNA in hepatocellular carcinoma. Hepatol Res 2015;45(2):128–141. doi:10.1111/hepr.12386, PMID:25040738.

[49] Ma T, Zhou X, Wei H, Yan S, Hui Y, Liu Y, *et al*. Long Non-coding RNA SNHG17 Upregulates RFX1 by Sponging miR-3180-3p and Promotes Cellular Function in Hepatocellular Carcinoma. Front Genet 2020;11:607636. doi:10.3389/fgene.2020.607636, PMID:33519911.

[50] Issac J, Raveendran PS, Das AV. RFX1: a promising therapeutic arsenal against cancer. Cancer Cell Int 2021;21(1):253. doi:10.1186/s12935-021-01952-6, PMID:33964962.

[51] Liu W, Wang B, Duan A, Shen K, Zhang Q, Tang X, *et al*. Exosomal transfer of miR-769-5p promotes osteosarcoma proliferation and metastasis by targeting DUSP16. Cancer Cell Int 2021;21(1):541. doi:10.1186/s12935-021-02257-4, PMID:34663350.

[52] Jing X, Xie M, Ding K, Xu T, Fang Y, Ma P, *et al*. Exosome-transmitted miR-769-5p confers cisplatin resistance and progression in gastric cancer by targeting CASP9 and promoting the ubiquitination degradation of p53. Clin Transl Med 2022;12(5):e780. doi:10.1101/2021.09.19.461013, PMID:35522909.